Article

J. Mex. Chem. Soc. **2010**, *54(2),* 111-116

ISSN 1870-249X

Isosteric Heats of Adsorption of N_2O and NO on Natural Zeolites

Gerardo Domínguez, Rosario Hernández-Huesca,* and Gelacio Aguilar-Armenta

Centro de Investigación de la Facultad de Ciencias Químicas, Benemérita Universidad Autónoma de Puebla, Blvd. 14 sur y Av. San Claudio, Ciudad Universitaria, C.P. 72570, Puebla, Pue. México, rosario.hernandez@fcquim.buap.mx

Received November 24, 2009; accepted May 25, 2010

Abstract. We studied the capacities of three natural zeolites to adsorb N_2O or NO using a glass high-vacuum volumetric system that permitted characterization of the energetics of the adsorption process. Adsorption equilibrium data were analyzed using the classical Freundlich equation and the Dual–Langmuir model. We employed the Clausius–Clapeyron relationship to calculate the isosteric heats of adsorption using the equilibrium data of the isotherms measured at 273.15 K and 293.15 K. The isosteric heats of reversible adsorption of both gases were smaller than the heats of total adsorption. The interaction energy of N_2O with mordenite was larger than the interaction energies of N_2O with either erionite or clinoptilolite. The interaction energy of NO was found to be largest with erionite.
Keywords: Adsorption, NOx, isosteric heats, natural zeolites.

Resumen. Estudiamos la capacidad que presentan tres zeolitas naturales de adsorber N_2O y NO, con el objetivo de obtener información sobre la energía característica del proceso de adsorción y mediante el uso de un sistema volumétrico al alto vacío. Las isotermas de adsorción de N_2O y NO se ajustaron a las ecuaciones de Dual-Langmuir y Freündlich, respectivamente. La ecuación de Clausius–Clapeyron se utilizó para calcular los calores isostéricos de adsorción a partir de las isotermas de adsorción medidas a 273.15 K y 293.15 K. El calor isostérico de la adsorción reversible de ambos gases presentó valores menores que los de la adsorción total. La energía de interacción del N_2O con mordenita fue mayor que con erionita y clinoptilolita, mientras que la energía de interacción de la molécula de NO fue mayor con erionita.
Palabreas clave: Adsorción, NOx, calores isostéricos, zeolitas naturales.

Introduction

The nitrogen oxides are predominantly emitted by the transportation industry and stationary industrial sources as gas flows containing the products of incomplete combustion. Without ignoring the production of nitric acid, atmospheric contamination by high concentrations of these oxides in emitted gases must be carefully considered. Nitrogen monoxide (NO) constitutes 95% of all the nitrogen oxide emissions [1], contributing in large measure to a variety of environmental problems such as acid rain and the resulting acidification of aquatic systems, high ozone levels and a general degradation in atmospheric visibility.

For these reasons, it is necessary to control nitrogen oxide. A simple method for the elimination of nitrogen oxides is the adsorption of these gases onto porous adsorbent materials. The method mentioned above allows them to be adsorbed and subsequently desorbed separately at different temperatures for their later treatment or direct application [2]. Another important function of these adsorbents is in concentrating the flows of some nitrogen oxides. A clear example of this is the selective recovery of N_2O on an adsorbent in order to produce a concentrated stream of the gas during the desorption. In fact, N_2O is a highly selective and valuable reactant in certain oxidation reactions [3]. Because zeolitic materials have a regular pore structure and high void volume, they are potentially practical solids with which to entrap large amounts of nitrogen oxides. The modification of these zeolites by ion exchange with metals can provide active sites that enhance selective adsorption.

A description of the energetics of gas adsorption necessitates an understanding of the binding behavior of a gas, in both pure and mixture forms, to the adsorbent. The isosteric heat of adsorption is an important parameter for describing the process of adsorption [2], and it is central to an understanding of gaseous mixture separation methods such as the pressure swing adsorption (PSA) method [4,5]. Optimization of the PSA method requires that the equilibrium quantities of an adsorbed substance be experimentally measured, as well as the absorption selectivity as a function of pressure, temperature, and composition [6].

The isosteric heat of adsorption depends on the extent of surface coverage because adsorbate–adsorbate interactions can alter the energetics of adsorption. In the context of physical adsorption, the interaction effects manifest as lateral van der Waals attractive forces between adsorbate molecules. Isosteric heats indicate the degree of adsorbent surface heterogeneity.

The isosteric heat of adsorption of a pure gas does not depend on the quantity of adsorbate on an energetically homogeneous surface. However, the isosteric heat of adsorption decreases with increasing quantities of adsorbed substances if the adsorbent surface is energetically heterogeneous due to the presence of several types of adsorption site. The isosteric heat can increase with increasing quantities of adsorbate when strong lateral interactions between adsorbed molecules are present [7].

It is difficult to experimentally measure the thermal properties of an adsorption process [8]; therefore, the heats of adsorption of pure gases are usually derived from adsorption isotherms using the Clapeyron equation. This study has examined the capacity of three natural zeolites, erionite (ERI), mordenite (MOR), and clinoptilolite (HEU) to adsorb N_2O and NO. The energetics of the adsorption process were characterized by evaluating the isosteric heats of adsorption of N_2O and NO calculated from the adsorption isotherms using the Clausius–Clapeyron equation.

Results and Discussion

Adsorption of N_2O

Figure 1 shows the adsorption isotherms of N_2O at 273.15 K with the different natural zeolites used in this study, which were fitted with Dual-Langmuir equation [9]:

$$a = \frac{a_{1m}K_1P}{1+K_1P} + \frac{a_{2m}K_2P}{1+K_2P} \quad (1)$$

In this figure it is observed that their adsorption capacities increase in the order HEU»MOR<ERI. Because the kinetic diameter of the N_2O molecule is 3.3 Å and clinoptilolite, mordenite, and erionite adsorb molecules with kinetic diameters that do not exceed 3.5, 3.9, and 4.3 Å, respectively [10], it is clear that adsorption of this gas is not influenced by esteric effects, and the adsorption behavior is mainly due to the limiting volume of the micropores [11] of the zeolites and the quantity of cations available per unit mass of the dehydrated zeolites (cationic density). The cationic density depends on the Si/Al ratio, which follows precisely the order HEU»MOR<ERI: clinoptilolites, 4.25 ≤ Si/Al ≤ 5.25; mordenites, 4.17 ≤ Si/Al ≤ 5.0; and erionites, 3 ≤ Si/Al 3.5 [10]. In other words, the adsorption capacity of ERI is greatest because there is a large amount of Al in this sample. Therefore, its cationic density is greater than that of the other two samples. The similar adsorption capacities of MOR and HEU is attributable to the similar Si/Al ratios and micropore volumes of the two zeolites.

The amount adsorbed irreversibly of N_2O was calculated by the difference between the total and reversible adsorption isotherm (Fig. 1) for this gas at a given temperature. The procedure to assess the extent of irreversible adsorbed amount was described in detail in a previous work [12]. An increase in irreversibility was observed in the order ERI<MOR»HEU in the range of all the equilibrium pressures studied (Table 1). The greatest proportion of irreversible adsorption shown by all three samples at low equilibrium pressures was due (in this range of pressures) to adsorption occurring at the most active adsorption sites (cations), at which desorption is most difficult because of the strong adsorbate–adsorbent interactions, as reflected in the value of Langmuir's constants K_1 and K_2 [9] (Table 2). In other words, the most active adsorption sites lead to a strong adsorbate-adsorbent interaction (K_1) being occupied at low equilibrium pressures, by reason of the desorption process is more difficult. Subsequently, at high equilibrium pressures the less active adsorption sites are occupied leading to a lower adsorbate-adsorbent interaction (K_2) and therefore to a lower irreversible adsorbed amount. Both, total and reversible adsorption isotherms of N_2O at 293.15 K were informed in a previous report [13].

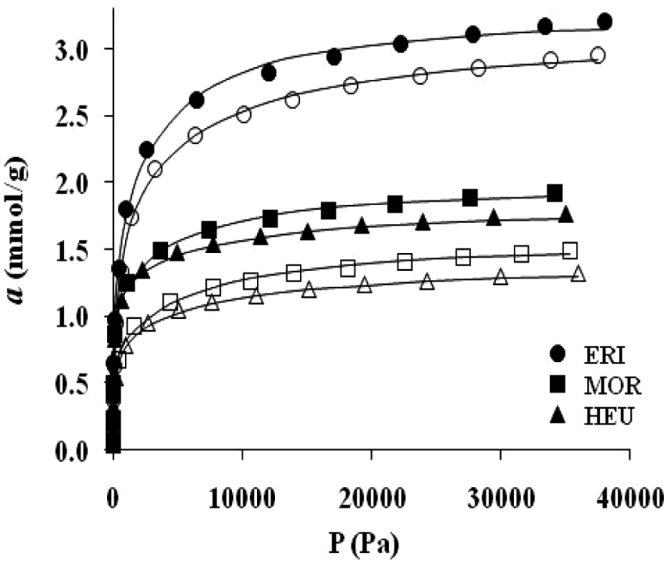

Fig. 1. Total (full symbols) and reversible (empty symbols) adsorption isotherms of N_2O at 273.15 K with natural zeolites. Symbols and continuous lines denote the experimental data and Dual-Langmuir model fit, respectively.

Isosteric heats of N_2O total adsorption

The isosteric heats of adsorption were computed from the equilibrium data measured at 273.15 K and 293.15 K, which had been fit to the Dual–Langmuir equation using a computational routine written in MATLAB [9]. At a constant level of adsorbate loading, the Clausius–Clapeyron relationship gives:

$$-\Delta H = Q_{st} = R\left[T_1T_2/(T_2-T_1)\right]\ln(P_2/P_1) \quad (2)$$

Figure 2 shows the isosteric heats of N_2O total adsorption for three zeolites as a function of the degree of coverage $\theta = a/a_m$. The total monolayer capacity ($a_m = a_{1m} + a_{2m}$) was calculated from the maximum quantity adsorbed on the adsorption

Table 1. Irreversibility grade for adsorption of N_2O at 273.15 K.

		ERI	MOR	HEU
Irreversibly (%)	800 Pa	13	34	36
	11332 Pa	9	26	27
	29998 Pa	8	23	25

Table 2. Optimal parameters for the Dual-Langmuir equation in fitting N_2O adsorption data at 273.15 K.

		ERI		MOR		HEU	
	Param number	1	2	1	2	1	2
Total	K (Pa^{-1})	0.012	0.0003	0.029	0.002	0.014	0.0002
	a_m (mmol/g)	1.36	1.95	1.05	0.95	1.21	0.64
Rev	K (Pa^{-1})	0.004	0.0002	0.018	0.0002	0.008	0.0002
	a_m (mmol/g)	1.71	1.44	0.73	0.87	0.80	0.6

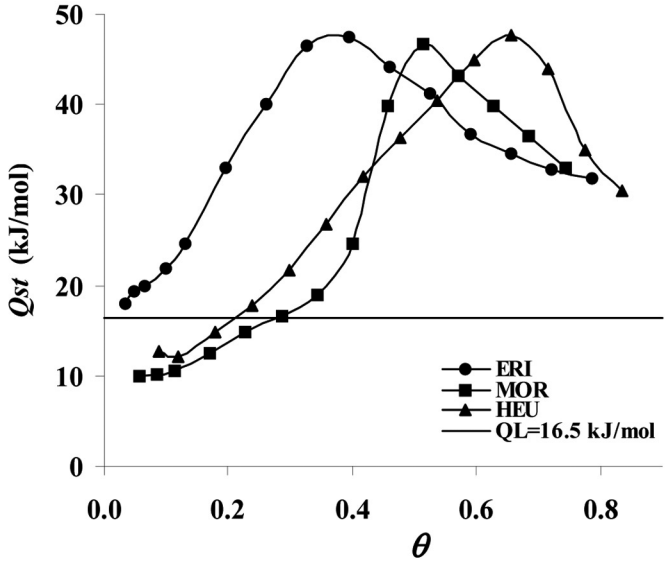

Fig. 2. Isosteric heats of total adsorption of N_2O with natural zeolites. Q_L is the latent heat of condensation.

sites 1 (a_{1m}) and 2 (a_{2m}) estimated using the Dual–Langmuir equation (1).

All three samples revealed isosteric heats of N_2O total adsorption that increased with increasing loading to a maximum value followed by a decrease, in agreement with previous reports [11,12,14-17]. This behavior indicated that both adsorbate–adsorbent and adsorbate–adsorbate interactions were present. The initial increase in the isosteric heat of total adsorption arose from the dominant adsorbate–adsorbate interactions, and the maximum indicated the presence of an energetically heterogeneous surface (adsorbate–adsorbent interactions). These results agreed with the fit to the Dual–Langmuir model for adsorption isotherms, i.e., at least two types of adsorption sites with different characteristic energies were present on the adsorbent surface. At low coverage, the monolayer was incomplete and the lateral interactions ($N_2O \leftrightarrow N_2O$) on the surface dominated. When θ tended to 1, i.e., when the monolayer nearly completely covered the surface, the adsorbate–adsorbent interactions dominated, decreasing in the isosteric heats of adsorption, which approached the latent heat of condensation (Q_L).

We note that a very low isosteric heat is expected at low surface coverage due to strong adsorbate–adsorbent interactions. However, the isosteric heat could not be accurately evaluated at such low levels of coverage using the isosteric heat method [18].

Isosteric heats of N_2O reversible adsorption

The aim of this study was to evaluate the influence of irreversible adsorption on the energetics of the adsorption process. Unlike the evaluation of the isosteric heat for total adsorption, this study examined the heat of adsorption in samples onto which N_2O had previously been irreversibly adsorbed. The results (Figs. 3–5) indicated that the quantity of irreversibly

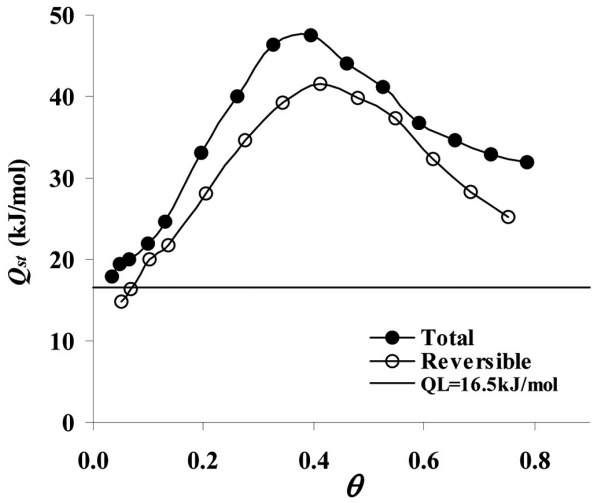

Fig. 3. Isosteric heats of adsorption of N_2O with ERI.

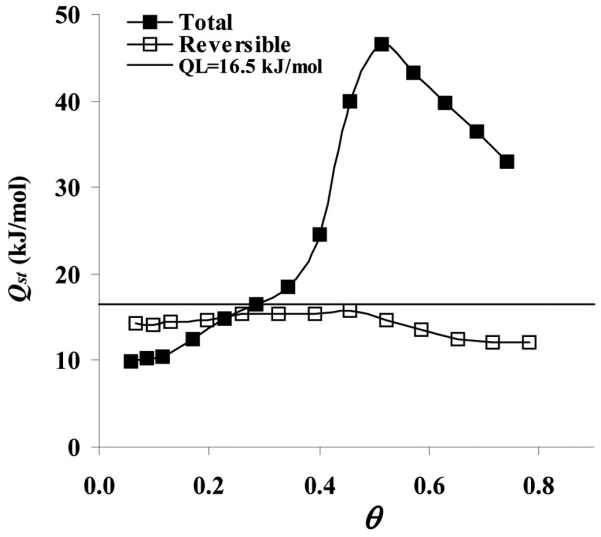

Fig. 4. Isosteric heats of adsorption of N_2O with MOR.

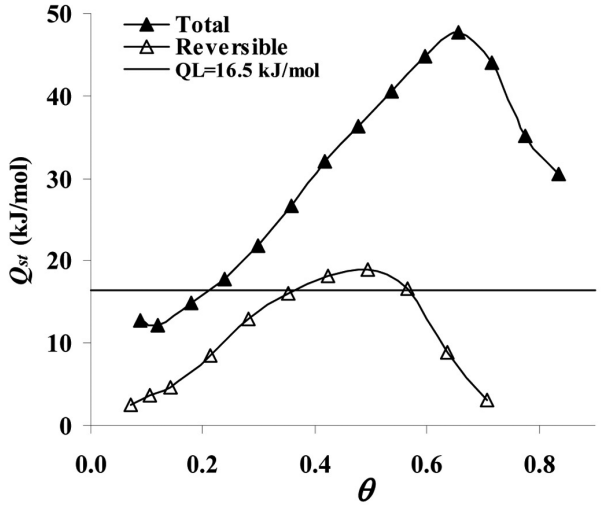

Fig. 5. Isosteric heats of adsorption of N_2O with HEU.

adsorbed molecules influenced the shape of the $Q_{st} = f(\theta)$ curve. The curve that described the isosteric heat of reversible adsorption was lower than the curve that described total adsorption in all three samples. This result indicated that during reversible adsorption, the most active adsorption centers were occupied by N_2O molecules. Therefore, the adsorbate–adsorbent interactions did not contribute greatly to the total interaction energy, thereby decreasing the total interaction energy. The decrease in the adsorbate–adsorbent interactions agreed well with the values of K_1 and K_2 obtained using the Dual–Langmuir equation for reversible adsorption (Table 2). That is, these constants decreased relative to those that described the total adsorption in all samples at both temperatures examined.

The ERI sample displayed a fraction of irreversible adsorption that was smaller than that of other samples (Table 1). Therefore, the heat of reversible adsorption in ERI was similar to the heat of total adsorption (Fig. 3). In contrast, the isosteric heats of total adsorption and reversible adsorption in the samples MOR and HEU (Figs. 4 and 5) showed important differences because these samples showed higher levels of irreversible adsorption (Table 1).

It should be emphasized that the isosteric heat of N_2O reversible adsorption in MOR remained constant (Fig. 4), suggesting that N_2O molecules were irreversibly adsorbed. Irreversible adsorption generated an energetically homogeneous surface, i.e., some N_2O molecules could not be desorbed because they occupied the most active adsorption sites. Therefore, reversible adsorption only occurred at one type of adsorption center. This result agreed with the fact that this sample displayed a value of K_1 that was much greater than that of other samples, and the heat of reversible adsorption was practically equal to the latent heat of evaporation of N_2O under conditions in which only dispersion forces were present, i.e., gas–solid interaction energies were low and yielded negligible contributions to the total interaction energy. At low surface coverage, the heat of adsorption for reversible adsorption was greater than the heat of total adsorption. This behavior could be neglected because the difference was very small and fell within the uncertainty limits of the isosteric method at low coverage, as mentioned above [18].

Adsorption of NO

As in the adsorption of N_2O, the capacities of these zeolite samples to adsorb NO at 273.15 K increases in the order MOR≈HEU<ERI (Fig. 6) in the range of all the equilibrium pressures studied. The fact that the cationic density of the zeolites also increases precisely in this order suggests the participation of cations as adsorptions centers for NO molecules, as Lunell et al. observed when they studied the adsorption of NO to the Na–Linde-type A (LTA) zeolite [19].

It is necessary to note that the adsorption of NO to all the samples was very slow. Because the kinetic diameter of the NO molecule is 3.17 Å, it is clear that the penetration of NO molecules into the micropores of the zeolites is not impeded,

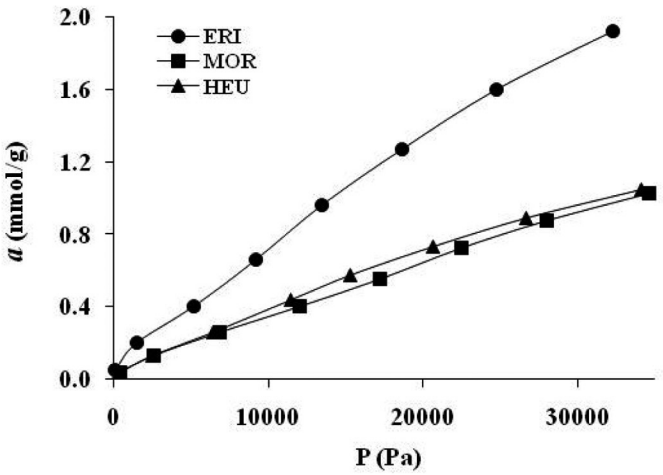

Fig. 6. Total adsorption isotherms of NO at 273.15 K with natural zeolites

but rather that the rate of diffusion of NO into the micropores is very slow. This may result from the formation of NO dimers inside the micropores, blocking the diffusion of further NO molecules into the same pores; i.e., the presence of the new N_2O_2 molecule would give rise to NO adsorption that is influenced by esteric effects.

The possible formation of the NO dimer is supported by the facts that the dimer exists in the liquid phase and its aggregation state in the liquid and adsorbed phases is similar. Furthermore, Biglino et al. demonstrated the existence of dimeric NO complexes in the LTA zeolite using pulse electronic paramagnetic resonance [20].

Analysis of the irreversible adsorption of NO revealed high irreversibility on all three adsorbents (Table 3). The greatest irreversibility was observed on ERI, possibly related to the greater number of dimeric NO complexes formed on this adsorbent (as a consequence of its greater adsorption of NO); the complexes could not be evacuated from the micropores during the desorption process at the employed temperature. This result may be attributable both to esteric effects and strong adsorbent–adsorbate interaction, as demonstrated by the theoretical constants n and K_H (Table 3) calculated from the Freundlich [21] and Henry [22] models, respectively. As a consequence of the high irreversibility and the major extent of adsorbent–adsorbate interaction present in ERI for total adsorption, during reversible adsorption it is ERI that shows the weakest adsorbent–adsorbate interaction of the three samples (Table 3). Both, total and reversible adsorption isotherms of NO at 293.15 K were reported in a previous work [13].

Isosteric heats of NO adsorption

The isosteric heats of adsorption were computed (via Eq. 2) from the equilibrium data measured at 273.15 and 293.15 K. These data fit well to the Freundlich and Henry equations.

Table 3. Irreversibility grade and n (Freundlich) and K_H (Henry) constants for adsorption of NO at 273.15 K.

Parameter / Adsorbent	Irreversibly (%)			n		K_H	
	800 Pa	11332 Pa	29998 Pa	Total	Tota	Rev	Rev
ERI	**85**	**75**	**58**	**1.47**	**0.96**	**0.0078**	**0.0036**
MOR	**79**	**68**	**65**	**1.27**	**1.07**	**0.0039**	**0.0015**
HEU	**70**	**57**	**52**	**1.28**	**1.08**	**0.0037**	**0.0018**

A decrease in the isosteric heat of total adsorption at low coverage was observed (Fig. 7) in all three samples, indicating that such conditions were dominated by adsorbate–adsorbent interactions. Figure 7 shows that the ERI sample displayed a marked decrease in the heat of adsorption relative to the heats of adsorption for the MOR and HEU samples. This behavior likely arose from the fact that the ERI sample showed greater irreversibility and higher values of n and K_H (Table 3) than did the other samples. Unlike the samples MOR and HEU, the isosteric heat of adsorption of ERI slightly increased with increasing a (for $a > 0.2$ mmol/g). This result may have arisen from the formation of NO dimers because, as mentioned, a greater quantity of dimers was observed to form on this sample.

We note that the isosteric heat curves for reversible adsorption were lower than the curves that described total adsorption in all three samples (e.g., Fig. 8) as consequence of the high levels of irreversible adsorption (Table 3).

Conclusions

Due to the differences in molecular weight, the levels of N_2O adsorption were higher than the levels of NO adsorption in all three adsorbents. Both gases were adsorbed in greater quantities in ERI than in MOR or HEU because ERI featured a higher cationic density and a higher micropore volume.

During total adsorption, N_2O molecules interacted more strongly with the surface of MOR than with other samples, generating an energetically homogeneous surface for reversible adsorption. In contrast, NO molecules interacted more strongly with the surface of ERI, yielding an initial decrease in the $Q_{st}=f(a)$ curve that was much greater for ERI than for the other samples.

Both gases displayed isosteric heats of reversible adsorption that were lower than the heats of total adsorption. It is possible that reversible adsorption was restricted to less active adsorption sites if the most active sites had been previously occupied by irreversibly adsorbed molecules during the total adsorption process.

Experimental

Three natural zeolites from various deposits in Mexico were used as adsorbents which, by simplicity, were named in the following way: Erionite (ERI), mordenite (MOR) and clinoptilolite (HEU).

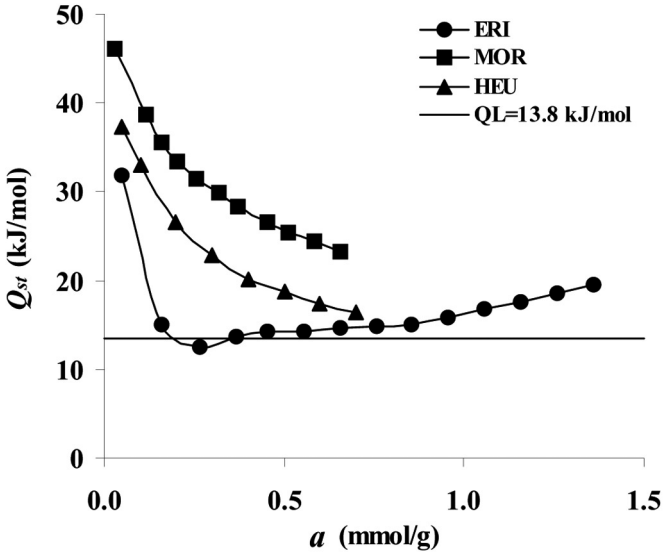

Fig. 7. Isosteric heats of total adsorption of NO with natural zeolites.

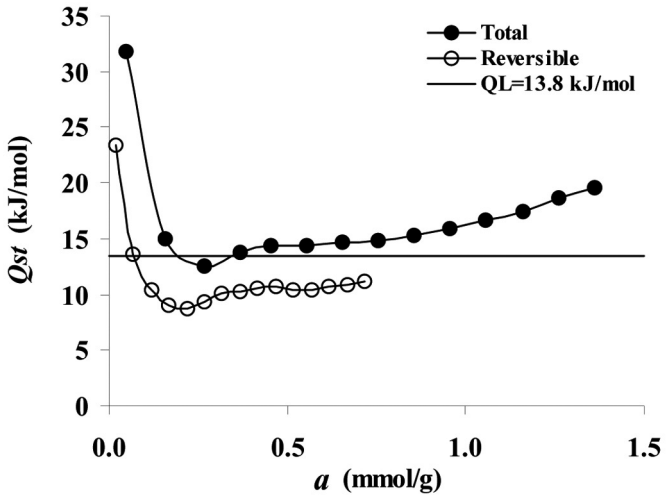

Fig. 8. Isosteric heats of adsorption of NO with ERI.

Characterization of the adsorbents

The adsorbents were characterized using the classic method of N_2 adsorption at 77 K and water adsorption at 293.15 K, as well by powder X-ray diffraction (XRD). Obtained results were informed in previous reports [11, 23].

Adsorption isotherms measurement

The adsorption isotherms were measured in a high vacuum volumetric system constructed entirely of Pyrex glass and equipped with teflon valves grease free. Vacuum was created by a mechanical pump E2M1.5 (Edwards) reaching residual pressures of 0.1333 Pa. Pressure was registered in a digital display pressure transducer TPR 017 (Balzers) for pressures in the interval of 133.32×10^{-4}-133.32 Pa, as well as in a pressure transducer CDG Gauge (Varian) Multi Gage digitally displayed for pressures that oscillate between 133.32 and 1.33332 x 10^5 Pa. Before the measurements were taken, around 500 mg of each one of the samples (fraction 0.38-0.54 mm) and were dehydrated in situ at 573.15 K in an oven constantly evacuating up to a residual pressure of 0.1333 Pa, having maintained these conditions for 3 h. Simultaneously, the determination of weight loss of the adsorbents was evaluated by heating samples to 573.15 K at atmospheric pressure in a conventional oven. After dehydration, temperature from the samples was reduced until reaching the temperature of measurement, and maintained constant during at least 1 h before starting any measurement. The 273.15 K temperature was obtained by using a bath of ice water.

The reversible adsorption isotherm was measured after obtaining total adsorption isotherm, previous evacuation of the sample to the temperature of measurement, until reaching residual pressures of 0.1333 Pa.

In order to check the reproducibility, some adsorption isotherms were measured three times (at different dates and with different batches). In all the cases the error rate obtained was less than 3%.

Acknowledgments

We are thankful to Consejo Nacional de Ciencia y Tecnología (CONACyT, Mexico) for financial support via scholarship No. 181781 and Project Ref. I36379-U.

References

1. Fritz, A.; Pitchon, V. *Appl. Catal., B* **1997,** *13,* 1-25.
2. Machida, M.; Uto, M.; Kurogi, D.; Kijima, T. *Chem. Mater*. **2000**, *12*, 3158-3164.
3. Centi, G.; Generali, P.; dall' Olio, L.; Perathorner, S. *Ind. Eng. Chem. Res*. **2000**, *39*, 131-137.
4. Hartzog, D. G.; Sircar, S. *Adsorption* **1995**, *1*, 133-151.
5. Sircar, S., in: "*Fundamentals of Adsorption, Proceedings of Engineering Foundation Conference held at Sonthofen*", Germany, Mersmann, A. B., et. al., Ed., Engineering Foundation, New York, **1991**, 815.
6. Siperstein, F.; Gorte, R. J.; Myers, A. L. *Langmuir* **1999**, *15*, 1570-1576.
7. Sircar, S.; Rao, M. B., in: *Surfaces of Nanoparticles in Porous Materials*, Schwarz, J.A., Contescu, C., Ed., Marcel and Dekker, New York, **1999**, 501-518.
8. Marchon, B.; Carrazza, J.; Heinemann, H.; Somorjai, G. A. *Carbon* **1998**, *26,* 507-514.
9. Do, D. D. *Adsorption Analysis: Equilibria and Kinetics*, Ed. Imperial College Press, Singapore, **1998**.
10. Breck, D.W. *Zeolite Molecular Sieves*, Ed. J. Wiley & Sons, Inc., New York, **1974**.
11. Hernández-Huesca, R.; Díaz, L.; Aguilar-Armenta, G. *Sep. Purif. Technol.* **1999**, *15*, 163-173.
12. Hernández-Huesca, R.; Aguilar-Armenta, G. *Rev. Soc. Quím. Méx.* **2002**, *46,* 109-114.
13. Hernández-Huesca, R.; Aguilar-Armenta, G.; Domínguez, G. *Sep. Sci. Technol.* **2009**, *44,* 63-74.
14. Sears, W. M. *Langmuir* **2001**, *17*, 5237-5244
15. Rakic, V., Dondur, V., Gajinov, S., Auroux, A. *Thermochim. Acta* **2004**, *420*, 51-57.
16. Patiño-Iglesias, M. E.; Aguilar-Armenta G.; Jiménez-Lopez, A.; Rodríguez-Castellon, E. *Colloids Surf. A* **2004**, *237*, 73-77.
17. Aguilar-Armenta, G.; Patiño-Iglesias, M. E.; Jiménez-Jiménez, J.; Rodríguez-Castellon, E.; Jiménez-Lopez, A. *Langmuir* **2006**, *22*, 1260-1267.
18. Rouquerol, F.; Rouquerol, J.; Sing, K. *Adsorption by Powders and Porous Solids*, Ed. Academic Press, London, **1999**.
19. Lunell, S.; Persson, P.; Lund, A.; Liu, Y.-J. *J. Phys. Chem. B* **2005**, *109,* 7948-7951.
20. Biglino, D.; Bonora, M.; Volodin, A.; Lund, A. *Chem. Phys. Lett.* **2001**, *349,* 511-516.
21. Freündlich, H. *Colloid and Capillary Chemistry*, Ed. Methuen, London, **1926**.
22. Guerasimov, Y.; Dreving, V. *Curso de Química Física*, Ed. MIR, Moscú, **1971**.
23. Aguilar-Armenta, G.; Patiño-Iglesias, M.E.; Leyva-Ramos, R. *Adsorpt. Sci. Technol.* **2003**, *21,* 81-91.